American Mineralogist, Volume 91, pages 1378–1384, 2006

Crystal chemistry and polytypism of tyrolite

Sergey V. Krivovichev,[1,2,*] Dmitrii Yu. Chernyshov,[3,4] Nicola Döbelin,[5] Thomas Armbruster,[5] Volker Kahlenberg,[2] Reinhard Kaindl,[2] Giovanni Ferraris,[6] Richard Tessadri,[2] and Gerard Kaltenhauser[2]

[1]Department of Crystallography, Faculty of Geology, St.Petersburg State University, St.Petersburg 199034, Russia
[2]Institut für Mineralogie und Petrographie, Universität Innsbruck, Innrain 52, A-6020 Innsbruck, Austria
[3]Swiss-Norwegian beamline, European Synchrotron Radiation Facility, BP 220, Grenoble 38043, France
[4]Petersburg Nuclear Physics Institute, St. Petersburg, Gatchina, 188350, Russia
[5]Laboratorium für chemische und mineralogische Kristallographie, Universität Bern, Freiestrasse 3, CH-3102 Bern, Switzerland
[6]Dipartimento di Scienze Mineralogiche e Petrologiche Università di Torino, 10125 Torino, Italy

Abstract

The crystal structures of the 1*M* and 2*M* polytypes of tyrolite have been solved from single-crystal X-ray diffraction data. The structure of tyrolite-1*M* [monoclinic, *P*2/*c*, *a* = 27.562(3), *b* = 5.5682(7), *c* = 10.4662(15) Å, β = 98.074(11)°, *V* = 1590.3(3) Å^3] has been refined to R_1 = 0.086 on the basis of 2522 unique observed reflections collected using synchrotron radiation at the Swiss-Norwegian beamline BM01 of the European Synchrotron Research Facility (SNBL at the ESRF). The structure of tyrolite-2*M* [monoclinic, *C*2/*c*, *a* = 54.520(6), *b* = 5.5638(6), *c* = 10.4647(10) Å, β = 96.432(9)°, *V* = 3154.4(6) Å^3] has been refined to R_1 = 0.144 on the basis of 2666 unique observed reflections obtained from a non-merohedrally twinned crystal using in-house X-ray radiation and a STOE IPDS II image-plate diffractometer. The structures are based upon complex nanolayers consisting of Cu, As, and Ca coordination polyhedra. The core of the nanolayer is a copper arsenate substructure consisting of **A** and **B** sublayers. The **B** sublayer consists of chains of edge-sharing Cu octahedra running along the *b* axis. The **A** sublayer contains trimeric units of Cu octahedra sharing corners with AsO_4 tetrahedra. Two adjacent **A** sublayers are linked by the octahedral chains of the **B** sublayer resulting in formation of the 18 Å thick **ABA** slab. The **ABA** slab is sandwiched between sublayers of Ca^{2+} cations and H_2O molecules. Adjacent nanolayers are connected by hydrogen bonds to the interlayer species (carbonate anions and H_2O molecules). The structures of tyrolite-1*M* and tyrolite-2*M* differ by the stacking sequence of the nanolayers only. The adjacent nanolayers in tyrolite-2*M* are shifted by *b*/2 = 2.8 Å in comparison to the relative position of the nanolayers in tyrolite-1*M*. The structural formula of tyrolite can be written as $[Ca_2Cu_9(AsO_4)_4(OH)_8(CO_3)(H_2O)_{11}](H_2O)_x$ where *x* = 0–1.

Keywords: Tyrolite, "clinotyrolite," crystal structure, copper arsenate, nanolayers, polytypes

Introduction

Copper arsenates are common minerals in oxidation zones of sulfide ore deposits. There are more than 70 different copper arsenate mineral species reported so far (see, e.g., recent papers: Pushcharovskii et al. 2000; Zubkova et al. 2003; Locock and Burns 2003). The restricted stability of As-bearing minerals such as the copper arsenates may play a significant role in the mobility of arsenic in the near-surface environment. Structural investigations of secondary As-bearing phases may lead to a better understanding of the geochemical behavior of As and thereby help to elucidate mechanisms of transportation and accumulation of As under natural conditions.

Tyrolite, a complex copper arsenate carbonate hydrate, was first described by A.G. Werner in 1817 (published in Haidinger 1845; cf. Blackburn and Dennen 1997) from Schwaz-Brixlegg, Tyrol, Austria. The mineral is widely distributed (Anthony et al. 2000) and has been reported at more than 128 localities worldwide.

On the basis of wet chemical analysis of material from Falkenstein, Austria, Church (1895) assigned the formula $CaCu_5(AsO_4)_2(CO_3)(OH)_4{\cdot}6H_2O$ to tyrolite. Berry (1948) reported tyrolite as orthorhombic, probable space group *Pmma*, *a* = 10.50, *b* = 54.71, *c* = 5.59 Å, *V* = 3211 Å^3, with *Z* = 4 and formula $Cu_9Ca_2(AsO_4)_4(OH)_{10}{\cdot}10H_2O$ (notably lacking any carbonate). Palache et al. (1951) considered the formula of tyrolite to be uncertain, particularly with respect to the presence or absence of carbonate and/or sulfate, and reported both previously cited formulae along with supporting chemical data. Guillemin (1956) assigned the formula $CaCu_5(AsO_4)_2(CO_3)(OH)_4{\cdot}6H_2O$ to tyrolite and considered the mineral as orthorhombic, space group *Pmma*, *a* = 10.212, *b* = 55.510, *c* = 5.602 Å, *V* = 3175.6 Å^3. Li et al. (2004) reported 0.73 wt% SO_3 in tyrolite from China. Castillo and Mallego (1972) provided chemical analysis of tyrolite with 7.17 wt% Fe_2O_3 and refined unit-cell dimensions as *a* = 10.48(5), *b* = 55.04(5), *c* = 5.57(5) Å. In 1980, Ma et al. reported occurence and properties of clinotyrolite, a tyrolite-like mineral with the composition $Cu_9Ca_2[(As,S)O_4]_4(OH,O)_{10}{\cdot}10H_2O$ and monoclinic symmetry, space group *Pa* or *P*2/*a*, *a* = 10.513, *b* = 5.56, and *c*

* E-mail: skrivovi@mail.ru

= 27.61 Å, β = 94.01°. Ma et al. (1980) pointed out that clinotyrolite is a monoclinic polymorph of tyrolite. Later, Liao et al. (1996) investigated the {001} surface structure of clinotyrolite using atomic force microscopy (AFM). Note that two varieties of tyrolite were first recognized by Müller (1979) in samples from Schwaz-Brixlegg, e.g., type locality of tyrolite. Schnorrer and Poeverlein (2002) described these two varieties as tyrolite and clinotyrolite and pointed out some differences in their color and crystal morphology.

Crystal structures of both tyrolite and clinotyrolite were previously unknown, primarily due to the poor quality of their platy and flexible crystals. Kloprogge and Frost (2000) reported a Raman spectrum of tyrolite from Schwaz-Brixlegg and reviewed the available spectroscopic data. Both the infrared and the Raman spectra of tyrolite suggest two symmetrically independent AsO_4^{3-} tetrahedra, OH^- groups, and H_2O molecules. Kloprogge and Frost (2000) assigned the bands around 1035 and 1088 cm^{-1} to the ν_1 modes of the CO_3^{2-} groups, but noted that this assignment is difficult because of overlap with the OH^- bending vibrations. Details of the crystal chemistry of tyrolite and clinotyrolite have remained unknown. The purpose of this study is to report the crystal structures of two tyrolite polytypes, which were solved using the experimental advantages provided by modern area detector technologies and high-intensity synchrotron radiation.

Experimental methods

The samples of tyrolite used in this study originate from the tyrolite type locality (Brixlegg, Schwaz, Tyrol). Sample T1 is from the personal collection of G.K., whereas sample T2 was taken from the mineralogical collections of the Institute of Mineralogy and Petrography of the University of Innsbruck.

Sample T1 represents a dolomite rock covered by greenish-blue flexible tyrolite crystals (Fig. 1a). All attempts to collect indexable X-ray diffraction data from relatively large crystals extracted from this sample were unsuccessful. In all cases, only two unit-cell parameters could be reliably determined, whereas the third could not be found. Close inspection of the sample T1 revealed two visually different aggregates: light blue plates and aggregates of greenish-blue elongated platy crystals. One of the greenish-blue aggregates was split and several strongly birefringent plates were selected under a polarizing microscope. X-ray diffraction experiments were performed under ambient conditions at the Swiss-Norwegian beamline BM01 of the European Synchrotron Research Facility (ESRF) using an imaging plate area detector (Mar345; 2300 × 2300 pixels) with a crystal-to-detector distance of 150 mm. Data were collected for the crystal with dimensions of 11 × 14 × 2 μm^3. Diffraction data were measured using monochromatized radiation (λ = 0.80000 Å) in an oscillation mode by rotating the crystal in ϕ by 2° in 2 min per frame; 179 frames were measured. The unit-cell parameters for the crystal T1 (Table 1) were found to be in general agreement with the unit-cell parameters reported by Ma et al. (1980) for clinotyrolite (see Introduction). The intensities were integrated and merged with the program CrysAlis. Lorentz and polarization corrections were applied; absorption effects were corrected using SADABS (based on the method of Blessing 1995). The structure was solved using SHELXS program. The agreement factor for the final model is $R_1 = 0.089$ for 2522 unique observed reflections with $|F_o| \geq 4\sigma_F$. The atomic coordinates and displacement parameters are given in Table 2.

Sample T2 represents a limestone with a small cavity filled with rectangular plates of tyrolite (Fig. 1b). One of the crystals was mounted on a glass fiber. X-ray diffraction data were collected by means of a STOE IPDS II diffractometer using monochromated Mo$K\alpha$ radiation and framewidths of 1° in ω. The unit-cell dimensions (Table 1) were refined by a least-squares technique. The unit-cell dimensions differ from those observed for the crystal extracted from sample T1. During data treatment, it was realized that the obtained diffraction pattern represents an overlap of two diffraction patterns corresponding to two twin components related by reflection on the (100) mirror plane. Figure 2a shows the reconstructed $h0l$ reciprocal space plot. Figure 2b provides the pattern obtained by superimposing two monoclinic reciprocal lattices related to each other by the (100) mirror plane. In both experimental pattern and calculated superimposed image, a pseudo-orthorhombic B-centered unit cell can be chosen; it corresponds to a supercell of the untwinned

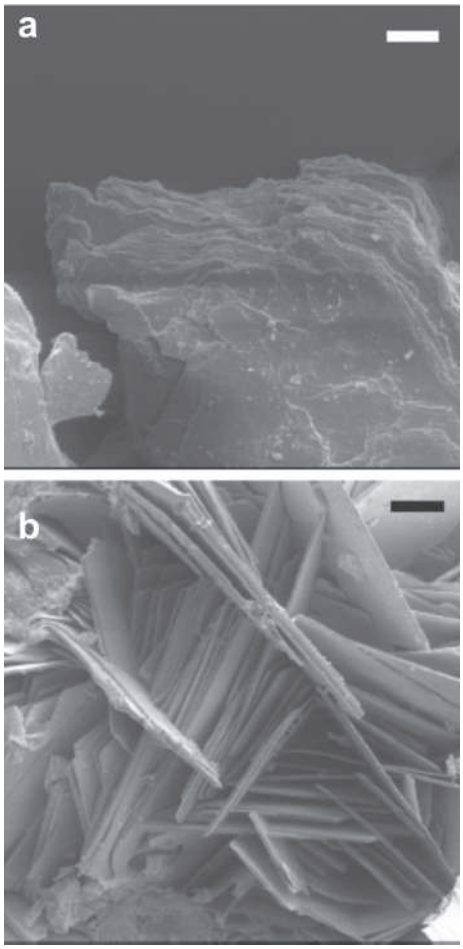

Figure 1. SEM photos of crystals of tyrolite-1M (**a**) and tyrolite-2M (**b**). Scale bars in the upper right parts of the photos correspond to 50 μm.

Table 1. Crystallographic data and refinement parameters for tyrolite-1M and tyrolite-2M

	tyrolite-1M	tyrolite-2M
a (Å)	27.562(3)	54.520(6)
b (Å)	5.5682(7)	5.5638(6)
c (Å)	10.4662(15)	10.4647(10)
β (°)	98.074(11)	96.432(9)
V (Å^3)	1590.3(3)	3154.4(6)
Space group	$P2/c$	$C2/c$
μ (cm^{-1})	10.477	10.570
Z	2	4
D_{calc} (g/cm^3)	3.302	3.327
Crystal size (μm)	0.014 × 0.011 × 0.002	0.18 × 0.12 × 0.03
λ (Å)	0.8000	0.71073
Total ref.	7795	11238
Unique ref.	2557	3116
Unique $\|F_o\| \geq 4\sigma_F$	2522	2666
R_{int}	0.059	0.109
R_σ	0.061	0.076
R_1	0.086	0.144
wR_2	0.241	0.359
S	1.128	1.085

Notes: $R_1 = \Sigma||F_o| - |F_c||/\Sigma|F_o|$; $wR2 = \{\Sigma[w(F_o^2 - F_c^2)^2]/\Sigma[w(F_o^2)^2]\}^{1/2}$; $w = 1/[\sigma^2(F_o^2) + (aP)^2 + bP]$, where $P = (F_o^2 + 2F_c^2)/3$; $s = \{\Sigma[w(F_o^2 - F_c^2)]/(n - p)\}^{1/2}$ where n is the number of reflections and p is the number of refined parameters.

TABLE 2. Atomic coordinates and displacement parameters for tyrolite-1*M*

Atom	*x*	*y*	*z*	U_{eq}	U_{11}	U_{22}	U_{33}	U_{23}	U_{13}	U_{12}
As1	0.86524(6)	−0.2818(3)	0.71749(16)	0.0098(5)	0.0205(9)	0.0037(8)	0.0062(9)	−0.0003(6)	0.0052(7)	0.0000(6)
As2	0.69328(6)	−0.6964(3)	0.79980(16)	0.0119(5)	0.0238(10)	0.0042(9)	0.0085(9)	0.0000(6)	0.0053(7)	−0.0007(7)
Cu1	0.76399(8)	−0.1650(4)	0.84020(19)	0.0121(5)	0.0222(11)	0.0096(11)	0.0051(10)	−0.0007(8)	0.0041(8)	0.0015(8)
Cu2	0.85745(8)	−0.1824(4)	0.02406(19)	0.0135(5)	0.0216(11)	0.0124(11)	0.0074(10)	−0.0039(8)	0.0049(8)	0.0014(8)
Cu3	0.94819(8)	−0.5359(4)	0.9187(2)	0.0132(5)	0.0258(12)	0.0069(11)	0.0073(10)	0.0002(8)	0.0041(8)	0.0035(8)
Cu4	0.76470(8)	−0.4692(4)	0.0984(2)	0.0123(5)	0.0231(12)	0.0049(10)	0.0102(11)	0.0025(8)	0.0065(8)	0.0013(8)
Cu5	0.0000	0.0000	0.0000	0.0183(8)	0.0387(19)	0.0088(15)	0.0081(15)	0.0002(12)	0.0055(13)	0.0070(13)
Ca	0.65147(13)	−0.2505(7)	0.9456(3)	0.0153(8)	0.0248(19)	0.0090(17)	0.0129(18)	−0.0003(14)	0.0052(14)	−0.0026(14)
O1	0.8339(4)	−0.294(2)	0.8477(12)	0.012(2)	0.019(6)	0.007(6)	0.012(6)	−0.007(5)	0.006(5)	0.000(5)
O2	0.8329(4)	−0.573(2)	0.0938(12)	0.016(3)	0.016(6)	0.012(6)	0.021(7)	0.002(5)	0.006(5)	0.002(5)
O3	0.9197(5)	−0.585(2)	0.2544(11)	0.015(3)	0.030(7)	0.012(6)	0.004(6)	0.000(5)	0.007(5)	−0.007(5)
O4	0.5928(5)	−0.423(3)	0.0623(14)	0.029(3)	0.037(8)	0.032(8)	0.021(7)	−0.003(7)	0.014(6)	−0.010(7)
O5	0.6363(6)	0.104(3)	0.0679(16)	0.034(4)	0.045(9)	0.016(7)	0.043(10)	0.007(7)	0.012(7)	0.002(7)
O6	0.8764(4)	−0.011(2)	0.1880(12)	0.014(3)	0.024(6)	0.003(5)	0.015(6)	−0.003(4)	0.003(4)	0.004(4)
O7	0.5876(6)	−0.095(4)	0.7893(16)	0.050(5)	0.047(10)	0.078(14)	0.026(9)	0.014(9)	0.003(7)	0.026(10)
O8	0.7032(4)	−0.326(2)	0.1443(11)	0.014(3)	0.019(5)	0.014(5)	0.011(5)	−0.006(5)	0.013(4)	−0.001(4)
O9	0.6352(5)	−0.617(2)	0.8116(12)	0.019(3)	0.030(7)	0.019(7)	0.011(6)	0.000(5)	0.013(5)	−0.002(6)
O10	0.9807(5)	−0.697(2)	0.0700(11)	0.015(3)	0.028(7)	0.012(6)	0.006(6)	0.004(5)	0.007(5)	0.000(5)
O11	0.9251(4)	−0.270(2)	0.0219(12)	0.016(3)	0.017(6)	0.015(6)	0.017(6)	−0.006(5)	0.004(5)	0.002(5)
O12	0.7270(5)	−0.498(2)	0.8955(12)	0.020(3)	0.040(8)	0.009(6)	0.009(6)	−0.002(5)	0.002(5)	−0.010(6)
O13	0.7023(5)	0.016(2)	0.8505(13)	0.017(3)	0.025(7)	0.007(6)	0.022(7)	0.002(5)	0.015(5)	0.000(5)
O14	0.7496(4)	−0.210(2)	0.6559(10)	0.010(2)	0.024(5)	0.005(5)	0.002(5)	0.001(4)	0.006(4)	−0.002(4)
O15	0.9704(5)	−0.844(2)	0.8322(12)	0.018(3)	0.033(7)	0.009(6)	0.014(6)	0.007(5)	0.007(5)	−0.001(5)
O16	0.7863(4)	−0.155(2)	0.0259(12)	0.012(2)	0.017(6)	0.003(5)	0.018(6)	0.002(5)	0.004(5)	−0.002(5)
O17*	0.8715(12)	0.207(6)	0.915(3)	0.037(7)	0.040(10)	0.037(11)	0.036(11)	0.012(9)	0.010(8)	0.000(8)
O18*	0.8060(8)	0.215(4)	0.820(2)	0.014(5)						
O19*	0.5057(16)	−0.075(8)	0.702(4)	0.062(11)						
O20*	0.4945(15)	−0.333(8)	0.018(4)	0.056(10)						
O21*	0.5303(16)	0.068(9)	0.885(4)	0.070†						
C1‡	0.5417(18)	−0.050(9)	0.791(4)	0.022(18)						

* s.o.f. = 0.50.
† Fixed during refinement.
‡ s.o.f. = 0.38(9).

crystal. Within this cell, non-space group absences occur if at the same time $H + 2K + L = 4n + 2$ and $H + 2K + 3L = 4n + 2$, where *HKL* are indices referred to the twin pseudo-orthorhombic cell. In direct space, this cell has approximate dimension of $a \approx 54.5$, $b \approx 5.6$, $c \approx 10.4$ Å, which is in general agreement with the parameters determined for tyrolite by Guillemin (1956). Thus, it is very likely that Guillemin (1956) has also studied a twinned crystal of tyrolite with the unit-cell dimensions similar to those of the crystal 2. Consequently, the unit cells given in the ICCD powder diffraction cards 2-0032 and 11-348 have to be revised. According to Ferraris et al. (2004), the twin observed in this sample of tyrolite can be described as twinning by reticular pseudomerohedry, obliquity 0.92°, twin index = 2. The two orientation matrices for the monoclinic twin components were used for intensity integration; however, it was impossible to separate diffraction patterns from the two twin components. Special care was taken to manually prepare a reflection file by selecting reflections, which could unambiguously be indexed and did not suffer from partial overlap, but all attempts failed to obtain better refinement quality. It should be noted that an exact overlap of the two monoclinic cells would occur if $a\cos\beta = c/2$; this condition is satisfied for $\beta = 95.51°$. The data were corrected for Lorentz, polarization, absorption, and background effects. The structure was solved by direct methods and refined by means of the program SHELX-97. At the final stage of the refinement, an additional twin model was introduced using the [–10–1/0–10/001] matrix, which improved the refinement. However, because of the numerous partial overlaps, the refinement quality was not perfect. A final agreement index (R_1) is 0.144, calculated for the 2666 unique observed reflections ($|Fo| > 4\sigma F$). The atomic coordinates and displacement parameters are given in Table 3. Selected bond lengths are listed in Table 4.

The structure models obtained for the crystals 1 and 2 have many features in common and differ only by the stacking sequence of the identical layers (see below). This allowed us (Guinier et al. 1984) to identify the studied species as two polytypes, tyrolite-1*M* (sample T1) and tyrolite-2*M* (sample T2). In the final refinements, atomic positions in both structures were renumbered to allow comparison of geometrical parameters of the two structures. As can be seen from Table 4, the bond lengths between the corresponding sites in the two structures are identical within 0.09 Å.

Raman spectra of tyrolite samples were recorded using the Jobin-Yvon Labpah-HR 800 spectrometer. The spectra were found to be in close agreement with those reported by Kloprogge and Frost (2000) and showed presence of carbonate and lack of any sulfate anions.

RESULTS

Cation coordination

There are five independent Cu positions in both structures. The Cu^{2+} cations are octahedrally coordinated by anions ($\phi = O^{2-}$, OH^-, H_2O). The $Cu^{2+}\phi_6$ octahedra are strongly distorted with four short (1.88–2.13 Å) and two long (2.21–2.91 Å) Cu^{2+}-ϕ bonds. This type of bond-length distortion is typical for the Cu^{2+} oxysalts owing to the Jahn-Teller effect (Jahn and Teller 1937; Burns and Hawthorne 1995); however, the observed distortions are also a function of ϕ as one can see from the different degree of distortion for the different Cu sites. The role of coordination is best illustrated for the most irregular $Cu^{2+}\phi_6$ octahedron observed for the Cu4 site. In both structures, the two apical (long) Cu^{2+}-ϕ bonds are highly irregular with one bond [Cu4-$\phi = O^{2-}$ (O12): 2.24 Å] being significantly shorter than the other [Cu4-$\phi = H_2O$ (O18): 2.82 Å]. It should be noted that the O17 and O18 sites represent H_2O molecules that are half-occupied. Thus coordinations of the Cu1, Cu2, Cu3, and Cu4 sites locally vary between distorted octahedral and square pyramidal.

Both tyrolite-1*M* and tyrolite-2*M* contain two symmetrically independent As sites tetrahedrally coordinated by four O atoms. The AsO_4^{3-} tetrahedra show typical geometries with the $As1O_4$ tetrahedron in the structure of tyrolite-2*M* being essentially compressed. However, it is not obvious whether this compression is due to structural effects or just a result of poor quality of the structure refinement.

Each structure contains one symmetrically independent Ca^{2+} site coordinated by five O atoms and two H_2O molecules.

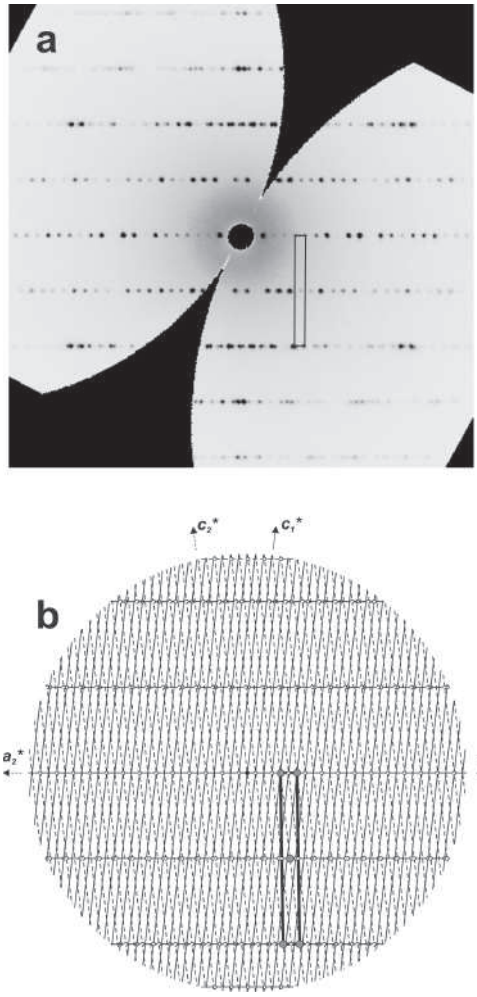

FIGURE 2. Reconstructed *h*0*l* reciprocal space plot from tyrolite-2*M* (**a**) and calculated pattern obtained by superposition of two monoclinic reciprocal lattices of tyrolite-2*M* related to each other by the (100) mirror plane (**b**). Empty circles correspond to the extinctions due to the *C*-centered monoclinic cells of the twin components.

Structure description

Figure 3 shows projection of the structure of tyrolite-1*M* along the *b* axis. It is based upon complex slabs consisting of Cu, As, and Ca coordination polyhedra. The slabs are about 26 Å = 2.6 nm thick and thus can be considered as nanolayers. This feature of the structure of tyrolite is very specific and has not been previously observed in oxysalt minerals. The architecture of the nanolayers can be understood in terms of separate sublayers. The core of the nanolayer is a copper arsenate substructure consisting of the **A** and **B** sublayers specified in Figure 3. The **B** sublayer represents a series of chains of edge-sharing Cu octahedra running along the *b* axis. Within the chain, three $Cu^{2+}\phi_6$ octahedra form trimers by sharing the common OH10 group (Fig. 4). Similar trimeric units constitute an important part of the **A** sublayer (Fig. 5). However, in this case, the trimers do not form chains but share corners with AsO_4 tetrahedra to produce complex 2-dimensional topology. The copper arsenate substructure consists of two **A** sublayers

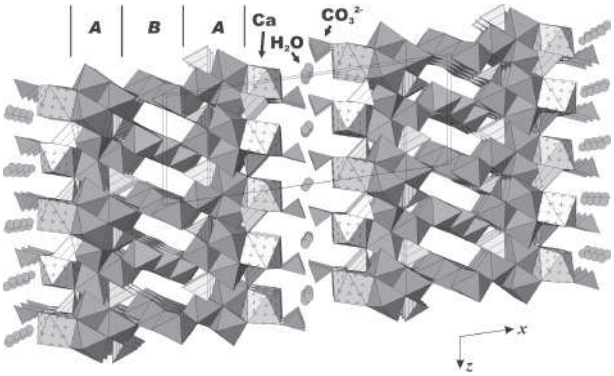

FIGURE 3. Projection of the crystal structure of tyrolite-1M along the *b* axis (perspective view). Legend: Cu octahedra = gray; As tetrahedra = lined; Ca polyhedra = cross-hatched. Note that in projections parallel to *b*, the 1*M* and 2*M* polytypes look very similar. However, both polytypes are distinct due to *b*/2 shifts of adjacent nanolayers.

linked by the octahedral chains from the **B** sublayer resulting in formation of the 18 Å thick **ABA** slab. The **ABA** copper arsenate slab is sandwiched between the sublayers of the Ca^{2+} cations and H_2O molecules. The adjacent nanolayers are connected by hydrogen bonds to the interlayer species (see below).

The structure of tyrolite-2*M* is very similar to that of tyrolite-1*M* and differs from the latter by the stacking sequence of the nanolayers.

Bond-valence analysis, interlayer species, and structural formula

Bond-valence analysis of the two structures was performed using bond-valence parameters taken from Brese and O'Keeffe (1991). The obtained bond-valence sums are listed in Table 5 together with the assignment of the anion positions to the O^{2-} and OH^- anions and H_2O molecules. The assignment made requires some additional comments.

The structure of the interlayer species has been resolved in the case of tyrolite-1*M* only. Even in this case, the interlayer components are significantly disordered. The interlayer contains approximately 50% occupied carbonate groups attached to the O7 site. For this reason, the occupancy of this site has been defined as $O_{0.5}H_2O_{0.5}$ (Table 5). There are also additional disordered positions that were assigned to the H_2O molecules, which most likely participate in hydrogen bonding between the nanolayers. We were unable to locate carbonate groups in the structure of tyrolite-2*M*. Instead, this structure contains a "ghost" peak Q (3.2 e^-) located at 1.47 Å from the O7 site. However, the interlayer sites may in fact correspond to low-occupied cationic species (e.g., low occupied Ca and/or Cu positions). However, the data quality does not allow unambiguous resolution of the interlayer content.

It should be noted that the bond-valence sum obtained for the O15 site is rather high for H_2O molecule (expected values for the H_2O-occupied site would be 0.00–0.40 v.u.). We suggest that the O15 site in fact accommodates OH-for-H_2O substitution that can be balanced by (1) H_2O-for-CO_3 substitution at the O7 site or (2) introduction of low-occupied cationic

TABLE 3. Atomic coordinates and displacement parameters for tyrolite-2*M*

Atom	*x*	*y*	*z*	U_{eq}	U_{11}	U_{22}	U_{33}	U_{23}	U_{13}	U_{12}
As1	0.06789(7)	0.2812(6)	0.3059(4)	0.0123(9)	0.015(2)	0.007(2)	0.014(2)	–0.0002(14)	0.0007(15)	–0.0005(13)
As2	0.15439(7)	0.3026(7)	0.0030(5)	0.0180(10)	0.020(2)	0.009(2)	0.026(2)	–0.0005(16)	0.0063(18)	0.0016(14)
Cu1	0.11904(9)	0.1678(8)	0.4956(5)	0.0158(10)	0.017(2)	0.015(2)	0.016(2)	0.0027(19)	0.006(2)	0.0016(18)
Cu2	0.07185(9)	0.8170(8)	0.1189(5)	0.0151(10)	0.019(2)	0.018(2)	0.009(2)	–0.0044(18)	0.0044(19)	–0.0018(18)
Cu3	0.02610(9)	0.5363(7)	0.4526(5)	0.0141(10)	0.024(2)	0.004(2)	0.014(2)	–0.0006(17)	0.001(2)	0.0046(17)
Cu4	0.11848(9)	0.5278(9)	0.2534(6)	0.0195(12)	0.017(2)	0.013(2)	0.028(3)	0.002(2)	0.001(2)	0.0003(19)
Cu5	0.0000	0.0000	0.0000	0.0205(16)	0.032(4)	0.011(3)	0.019(4)	–0.003(3)	0.005(3)	–0.010(3)
Ca	0.1753(2)	0.7487(15)	0.1761(9)	0.0231(19)	0.035(5)	0.015(4)	0.020(5)	0.006(3)	0.005(4)	0.002(3)
O1	0.0831(4)	0.295(5)	0.455(3)	0.012(5)						
O2	0.0841(5)	0.431(5)	0.201(3)	0.017(6)						
O3	0.0404(4)	0.417(4)	0.300(3)	0.009(5)						
O4	0.2056(7)	0.582(7)	0.338(4)	0.043(9)						
O5	0.1829(7)	0.106(7)	0.286(4)	0.043(9)						
O6	0.0624(5)	0.003(5)	0.270(3)	0.020(6)						
O7	0.2086(8)	0.892(9)	0.053(5)	0.057(12)						
O8	0.1495(5)	0.320(5)	–0.163(3)	0.014(5)						
O9	0.1836(6)	0.379(6)	0.062(3)	0.028(7)						
O10	0.0092(6)	0.299(6)	0.073(4)	0.029(7)						
O11	0.0378(5)	0.273(5)	0.576(3)	0.022(6)						
O12	0.1372(5)	0.500(6)	0.075(3)	0.025(7)						
O13	0.1500(5)	0.011(5)	0.049(3)	0.019(6)						
O14	0.1265(4)	0.211(4)	0.323(3)	0.011(5)						
O15	0.0147(5)	0.146(5)	–0.151(3)	0.019(6)						
O16	0.1078(5)	0.843(5)	0.167(3)	0.015(6)						
O17*	0.0678(11)	0.195(11)	0.012(6)	0.024(13)						
O18*	0.0981(10)	–0.207(10)	0.455(6)	0.018(12)						
O19*	0.247(3)	0.56(3)	0.091(19)	0.14(6)						
O20*	0.248(2)	0.17(2)	0.149(12)	0.08(3)						
O21†	0.256(5)	0.79(5)	0.06(3)	0.080§						
Q‡	0.2352(17)	0.852(17)	0.043(11)	0.050						

* s.o.f. = 0.50.
† s.o.f. = 0.21(11).
‡ Peak height = 3.2(1) e^-.
§ Fixed during refinement.

species into the interlayer. Once again, this problem cannot be resolved using the present data quality.

Taking into account the results of structural investigation and the discussion presented above, the structural formula of tyrolite can be written as $[Ca_2Cu_9(AsO_4)_4(OH)_8(CO_3)(H_2O)_{11}](H_2O)_x$ where $x = 0–1$. This formula is in good agreement with the H_2O amount determined for tyrolite by Guillemin (1956) as 12 H_2O molecules per 4 As atoms. However, the Ca:Cu:As ratio was determined by Guillemin (1956) as 1:5:2, whereas the correct ratio is 2:9:4, as found by Berry (1948) for tyrolite and by Ma et al. (1980) for clinotyrolite.

Presumably the clinotyrolite of Ma et al. (1980) corresponds to tyrolite-1*M* described in this paper; however, without a structural study of the holotype samples, which contain S as well, it is impossible to reach a firm conclusion.

DISCUSSION

The structures of tyrolite-1*M* and tyrolite-2*M* differ by the stacking sequence of the nanolayers. In both structures, adjacent nanolayers are translationally equivalent. The adjacent nanolayers in tyrolite-2*M* are shifted by $b/2 = 2.8$ Å in comparison to the relative position of the nanolayers in tyrolite-1*M*. This shift is quite subtle compared to the thickness of the nanolayers (26 Å). Perhaps, this feature of the tyrolite polytypes explains the difficulties associated with the structural characterization of this mineral. Most of the tyrolite crystals that we studied were unindexable along the direction perpendicular to the nanolayers. This could be the result of the loss of periodicity along the *a* axis due to the presence of extensive stacking faults or the loss

TABLE 4. Selected bond lengths (Å) in the structures of tyrolite-1*M* and tyrolite-2*M*

	1*M*	2*M*		1*M*	2*M*
As1-O3	1.670(12)	1.67(2)	Cu4-O14	1.951(12)	1.94(3)
As1-O2	1.674(12)	1.70(3)	Cu4-O2	1.972(12)	1.97(3)
As1-O6	1.694(12)	1.62(3)	Cu4-O8	1.991(12)	2.00(3)
As1-O1	1.715(12)	1.69(3)	Cu4-O16	2.029(12)	2.03(3)
<As1-O>	1.69	1.67	Cu4-O12	2.235(13)	2.23(3)
			Cu4-O18	2.82(2)	2.90(6)
As2-O12	1.681(12)	1.67(3)	<Cu4-ϕ>	2.17	2.18
As2-O9	1.682(13)	1.70(3)			
As2-O13	1.692(12)	1.72(3)	Cu5-O10	1.945(13)	1.88(3)
As2-O8	1.693(11)	1.73(3)	Cu5-O10	1.945(13)	1.88(3)
<As2-O>	1.69	1.70	Cu5-O15	2.026(12)	2.02(3)
			Cu5-O15	2.026(12)	2.02(3)
Cu1-O14	1.930(11)	1.91(3)	Cu5-O11	2.589(13)	2.61(3)
Cu1-O16	1.955(12)	1.96(3)	Cu5-O11	2.589(13)	2.61(3)
Cu1-O13	1.995(12)	1.99(3)	<Cu5-ϕ>	2.19	2.17
Cu1-O1	2.046(12)	2.08(2)			
Cu1-O12	2.231(13)	2.21(3)	Ca-O13	2.356(12)	2.32(3)
Cu1-O18	2.43(2)	2.39(6)	Ca-O4	2.365(14)	2.42(4)
<Cu1-ϕ>	2.10	2.09	Ca-O8	2.388(13)	2.34(3)
			Ca-O7	2.392(16)	2.47(5)
Cu2-O11	1.932(12)	1.93(3)	Ca-O5	2.420(16)	2.31(4)
Cu2-O16	1.969(12)	1.97(3)	Ca-O9	2.483(14)	2.45(3)
Cu2-O1	1.969(12)	1.98(3)	Ca-O12	2.611(15)	2.62(3)
Cu2-O6	1.970(12)	2.00(3)	<Ca-ϕ>	2.43	2.42
Cu2-O2	2.420(13)	2.38(3)			
Cu2-O17	2.51(3)	2.38(7)	C-O21	1.26(2)	n/d
<Cu2-ϕ>	2.13	2.11	C-O19	1.27(7)	n/d
			C-O7	1.29(5)	n/d
Cu3-O3	1.910(12)	1.97(3)	<C-O>	1.27	
Cu3-O10	1.927(12)	1.88(3)			
Cu3-O11	1.989(13)	2.01(3)			
Cu3-O15	2.071(13)	2.13(3)			
Cu3-O10	2.339(13)	2.32(3)			
Cu3-O17	2.55(3)	2.73(6)			
<Cu3-ϕ>	2.13	2.17			

Note: ϕ = O, OH, H_2O.

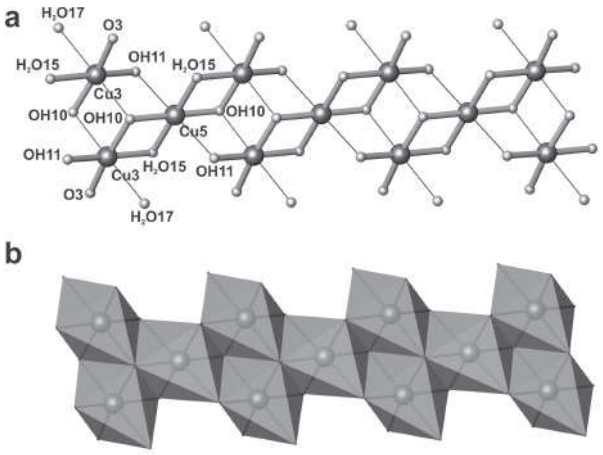

FIGURE 4. Ball-and-stick (**a**) and polyhedral (**b**) representations of the chain of edge-sharing Cu octahedra that constitute the **B** sublayer of the structure of tyrolite polytypes.

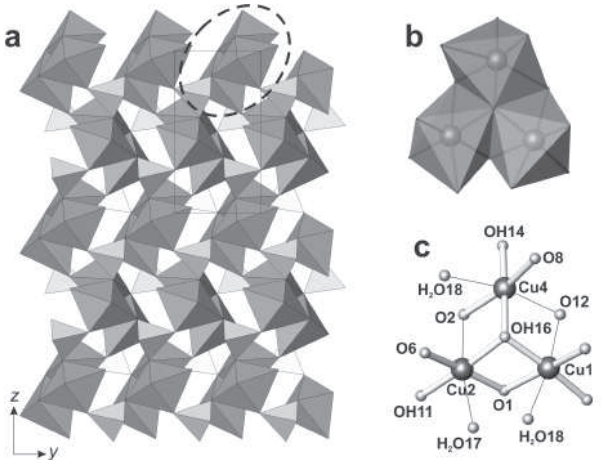

FIGURE 5. Sublayer A projected onto (100) plane (**a**) (Cu polyhedra = dark gray; As tetrahedra = light gray) and polyhedral (**b**) and ball-and-stick (**c**) representations of trimeric unit of Cu octahedra.

of structural integrity.

The unique character of the structures of tyrolite polytypes described here (nanometer-sized layers linked by weak hydrogen bonds) makes it interesting from the viewpoint of material science. Recently, layered materials with weak interlayer bonding have attracted considerable attention. These materials can be exfoliated into nanosheets with subsequent fabrication of nanomaterials (e.g., by rolling nanosheets into nanotubes or by intercalating of organic molecules in between the layers and fabrication of organic/inorganic nanocomposites) (Ma et al. 2004). Tyrolite polytypes are especially interesting in this regard owing to the magnetism of the Cu^{2+} cations. In tyrolites, a 2-dimensional nanosized substructure of transition metal ions (Cu^{2+}) is sandwiched between the layers of dielectric Ca^{2+} cations and H_2O molecules. This peculiarity of the tyrolite structure makes it very interesting from the viewpoint of physical properties, which are currently under investigation. It is also generally known

TABLE 5. Bond-valence sums for atoms in the structures of tyrolite-1*M* and tyrolite-2*M*

Atom	1*M*	2*M*	Site assignment
As1	5.26	5.57	As
As2	5.27	5.06	As
Cu1	2.13	2.16	Cu
Cu2	2.11	2.09	Cu
Cu3	2.09	2.01	Cu
Cu4	2.02	2.00	Cu
Cu5	1.93	2.06	Cu
Ca	2.05	2.12	Ca
O1	2.05	2.11	O
O2	1.94	1.88	O
O3	1.92	1.84	O
O4	0.34	0.30	H_2O
O5	0.29	0.39	H_2O
O6	1.75	2.00	O
O7*	0.32/1.63	0.25	$O_{0.5}H_2O_{0.5}$
O8	1.85	1.98	O
O9	1.59	1.54	O
O10	1.17	1.33	OH
O11	1.02	1.01	OH
O12	1.96	2.01	O
O13	1.73	2.04	O
O14	0.99	1.03	OH
O15†	0.74	0.69	H_2O
O16	1.32	1.32	OH
O17	0.20	0.19	H_2O
O18	0.18	0.19	H_2O
O19	1.38*	–	O in 1*M*; H_2O in 2*M*
O20	–	–	H_2O
O21	1.42*	–	O in 1*M*; H_2O in 2*M*

* Attached to the 50% occupied C^{4+} site.
† The bond-valence sum is rather high. See text for details.

that physical properties of nanosized particles are enhanced in comparison to the macroscopic crystals [see, e.g., recent report of Sigman and Korgel (2005) on optical anisotropy of mendipite ($Pb_3O_2Cl_2$) nanobelts].

ACKNOWLEDGMENTS

We thank Andrew Locock (Toronto) and Natalia V. Zubkova (Moscow) for many useful and detailed comments that significantly improved the manuscript. S.V.K. thanks the Austrian Science Fund (FWF) (grant no. M771-N10) and Russian Ministry of Science and Education (grant 2.1.1.3077) for financial support. We are grateful to L. Liao (China University of Geosciences, Beijing) for providing us with the reprint of the paper on the AFM study of clinotyrolite. We thank V. Dmitriev and P. Pattison for the assistance during synchrotron experiments in Grenoble. Thilo Arlt (formerly Bern) is thanked for making X-ray single-crystal photographs of twinned tyrolite-2*M* available to us.

REFERENCES CITED

Anthony, J.W., Bideaux, R.A., Bladh, K.W., and Nichols, M.C. (2000) Handbook of Mineralogy,Volume IV, Arsenates, Phosphates, Vanadates. Mineral Data Publishing, Tucson.

Berry, L.G. (1948) Tyrolite, higginsite, and cornwallite. American Mineralogist, 33, 193.

Blackburn, W.H. and Dennen, W. H. (1997) Encyclopedia of Mineral Names. The Canadian Mineralogist, Special Publication 1.

Blessing, R.H. (1995) An empirical correction for absorption anisotropy. Acta Crystallographica, A51, 33–38.

Brese, N.E. and O'Keeffe, M. (1991) Bond-valence parameters for solids. Acta Crystallographica, B47, 192–197.

Burns, P.C. and Hawthorne, F.C. (1995) Coordination geometry structural pathways in Cu^{2+} oxysalt minerals. Canadian Mineralogist, 33, 889–905.

Castillo, R.A. and Mallego, M.R. (1972) Tyrolite from Molvizar (Granada). Cuadernos de Geologia, Universidad de Granada, 3(1), 41–47.

Church, A.H. (1895) A chemical study of some native arsenates and phosphates. Mineralogical Magazine, 11, 1–12.

Ferraris, G., Mackovicky, E., and Merlino, S. (2004) Crystallography of Modular Materials. IUCr Monograph in Crystallography, Oxford University Press, U.K.

Guillemin, C. (1956) Contribution a la mineralogie des arsenates, phosphates et

vanadates de cuivre. Bulletin de la Société Française de Minéralogie et de la Cristallographie, 79, 7–95.

Guinier, A., Bokij, G.B., Boll-Dornberger, K., Cowley, J.M., Durovic, S., Jagodzinski, H., Krishna, P., De Wolff, P.M., Zvyagin, B.B., Cox, D.E., Goodman, P., Hahn, Th., Kuchitsu, K., and Abrahams, S.C. (1984) Nomenclature of polytype structures, report of the International Union of Crystallography *Ad-Hoc* Committee on the nomenclature of disordered, modulated and polytypestructures. Acta Crystallographica, A40, 399–404.

Haidinger, W. (1845) Handbuch der bestimmenden Mineralogie. Wien.

Jahn, H.A. and Teller, E. (1937) Stability of polyatomic molecules in degenerate electronic states. Proceedings of the Royal Society, Series A, 161, 220–235.

Kloprogge, J.T. and Frost, R.L. (2000) Raman microscopy study of tyrolite: a multi-anion arsenate mineral. Applied Spectroscopy, 54, 517–521.

Li, Y., Lai, L., Zhou, W., and Qin, C. (2004) Mineralogical characteristics and geological significance of tyrolite. Kuangwu Xuebao, 24(4), 378–380.

Liao, L., Ma, Z., and Shi, N. (1996) {001} surface structure of clinotyrolite revealed by atomic force microscope (AFM). Chinese Science Bulletin, 41, 759–761.

Locock, A.J. and Burns, P.C. (2003) Crystal structures and synthesis of the copper-dominant members of the autunite and meta-autunite groups: torbernite, zeunerite, metatorbernite, and metazeunerite. Canadian Mineralogist, 41, 489–502.

Ma, R., Bando, Y., and Takayoshi, S. (2004) Directly rolling nanosheets into nanotubes. Journal of Physical Chemistry, B108, 2115–2119.

Ma, Z.-S., Qian, R.-Y., and Peng, Z.-Z. (1980) Clinotyrolite—a new hydrous copper arsenate mineral discovered in Dongchuan, Yunnan [China]. Dizhi Xuebao, 54, 134–143.

Müller, E. (1979) Primäre und sekundäre Kupferminerale am Gratlspitz bei Brixlegg, Tirol. Karinthin, 80, 99–104.

Palache, C., Berman, H., and Frondel, C. (1951) Dana's System of Mineralogy, 7th edition, p. 925–926. John Wiley and Sons, New York.

Pushcharovskii, D.Yu., Teat, S.J., Zaitsev, V.N., Zubkova, N.V., and Sarp, H. (2000) Crystal structure of pushcharovskite. European Journal of Mineralogy, 12, 95–104.

Schnorrer, G. and Poeverlein, R. (2002) Schwaz-Brixlegg-Fundstellen: 2. Die Minerale des Stockerstollens bei Brixlegg in Tirol. Aufschluss, 53, 209–228.

Sigman, M.B., Jr. and Korgel, B.A. (2005) Strongly birefringent $Pb_3O_2Cl_2$ nanobelts. Journal of the American Chemical Society, 127, 10089–10095.

Zubkova, N.V., Pushcharovskii, D.Yu., Sarp, H., Teat, S.J., and MacLean, E.J. (2003) Crystal structure of zdenekite $NaPbCu_5(AsO_4)_4 \cdot 5(H_2O)$. Crystallography Reports, 48, 939–943.

MANUSCRIPT RECEIVED JULY 20, 2005
MANUSCRIPT ACCEPTED APRIL 7, 2006
MANUSCRIPT HANDLED BY MARTIN KUNZ